JOURNAL OF GEOPHYSICAL RESEARCH, VOL. 113, C04008, doi:10.1029/2006JC003979, 2008

A 170-year Sr/Ca and Ba/Ca coral record from the western Pacific warm pool: 1. What can we learn from an unusual coral record?

Chantal Alibert[1] and Leslie Kinsley[1]

Received 17 October 2006; revised 25 September 2007; accepted 30 October 2007; published 9 April 2008.

[1] A long-lived *Porites* coral from New Ireland (2.5°S, 150.5°E), Papua New Guinea, has been analyzed for Sr/Ca and Ba/Ca by laser ablation inductively coupled plasma mass spectrometry (LA-ICPMS). The top 50 years of the core are examined here and compared with instrumental sea surface temperatures (SSTs). For the small range of SST in the warm pool, Sr/Ca shows an unusually large response. The best estimate for the slope of a temperature calibration is −0.23 ± 0.03 mmol/mol per°C. This strong slope is partly a result of the high-resolution sampling, but is also due to additional biological mediation of the Sr/Ca ratios, which appears to be associated with seasonal changes of calcification rate, and limits the prediction skills of this proxy thermometer. High-density bands synchronous with high Sr/Ca ratios suggest that calcification may be enhanced by beneficial small amounts of nutrients available during El Niño. Transient Ba enrichment, synchronous with colder than average SST, is also observed during El Niño and attributed to the shoaling of the New Ireland Coastal Undercurrent. The high level of enrichment, in particular during upwelling triggered by westerly wind bursts, suggests an origin from both dissolved seawater and marine biological barium.

Citation: Alibert, C., and L. Kinsley (2008), A 170-year Sr/Ca and Ba/Ca coral record from the western Pacific warm pool: 1. What can we learn from an unusual coral record?, *J. Geophys. Res.*, *113*, C04008, doi:10.1029/2006JC003979.

1. Introduction

[2] During the past decade, massive corals have been increasingly used to extract valuable multicentury climate records, mainly using oxygen isotopes. For example, the Maiana coral from the central Pacific records ENSO-related variations of δ^{18}O [*Urban et al.*, 2000] and extends the rainfall record of equatorial Pacific islands back to 1840, while the δ^{18}O composition of corals from New Caledonia [*Quinn et al.*, 1998] is mainly recording sea surface temperatures (SST). There are as yet only a few coral records for the western Pacific warm pool, where there is little instrumental temperature data extending back more than ∼50 years. *Quinn et al.* [2006] have recently reported δ^{18}O and Sr/Ca compositions for a coral at Rabaul (4°S, 152°E), which mainly record the cooling accompanying the El Niño events back to the 1870s.

[3] We report on a 170-year record of Sr/Ca and Ba/Ca variations of a *Porites* coral from Kavieng (150.5°E, 2.5°S), in the New Ireland province of Papua New Guinea (Figure 1), analyzed by laser ablation inductively coupled plasma mass spectrometry (LA-ICPMS). In this first part, the top 50 years of the coral are examined, with the aim to understand the environmental significance of Sr/Ca and Ba/Ca variations.

2. Analytical Methods and Climatic Data Sets

[4] Three *Porites* coral heads were sampled in April 1997 around Kavieng, the first one off the northeast pass north of Lavongai, dubbed “NEP”, the second one in the main channel near Lemus Island (“LEM”) and the third one off Steffen Strait, facing the Bismarck Sea (“STE”). Surface seawater was also sampled at four locations. Coral cores, obtained using a hydraulic drill that produces cores 70 cm long and 7 cm in diameter, were sliced at 6 mm thickness and X rays were taken for each slice. The top part of each coral core was sampled for Sr/Ca analysis by isotope dilution thermal ionization mass spectrometry (TIMS) using a mixed ^{43}Ca-^{84}Sr spike, as previously described [*Alibert et al.*, 2003]. Samples were taken with a microdrill every 0.5 mm, from a 2 mm thick ledge, to a depth of 1 mm, giving ∼1 mm^3 of coral powder. Each coral colony revealed a distinct pattern of Sr/Ca variations that proved difficult to match to SSTs (Figure S1[1]) [*Alibert*, 1999]. To try to understand these puzzling data, we extended our investigation to other trace elements using LA-ICPMS. Only the NEP coral was selected, on the basis of its open ocean environment, and periodic covariations of Sr/Ca, U/Ca and Mg/Ca, likely to be annual. It is a gray blue, bell-shaped

[1]Research School of Earth Sciences, Australian National University, Australia.

0148-0227/08/2006JC003979$09.00

[1]Auxiliary material data sets are available at ftp://ftp.agu.org/apend/jc/2006jc003979. Other auxiliary material files are in the HTML.

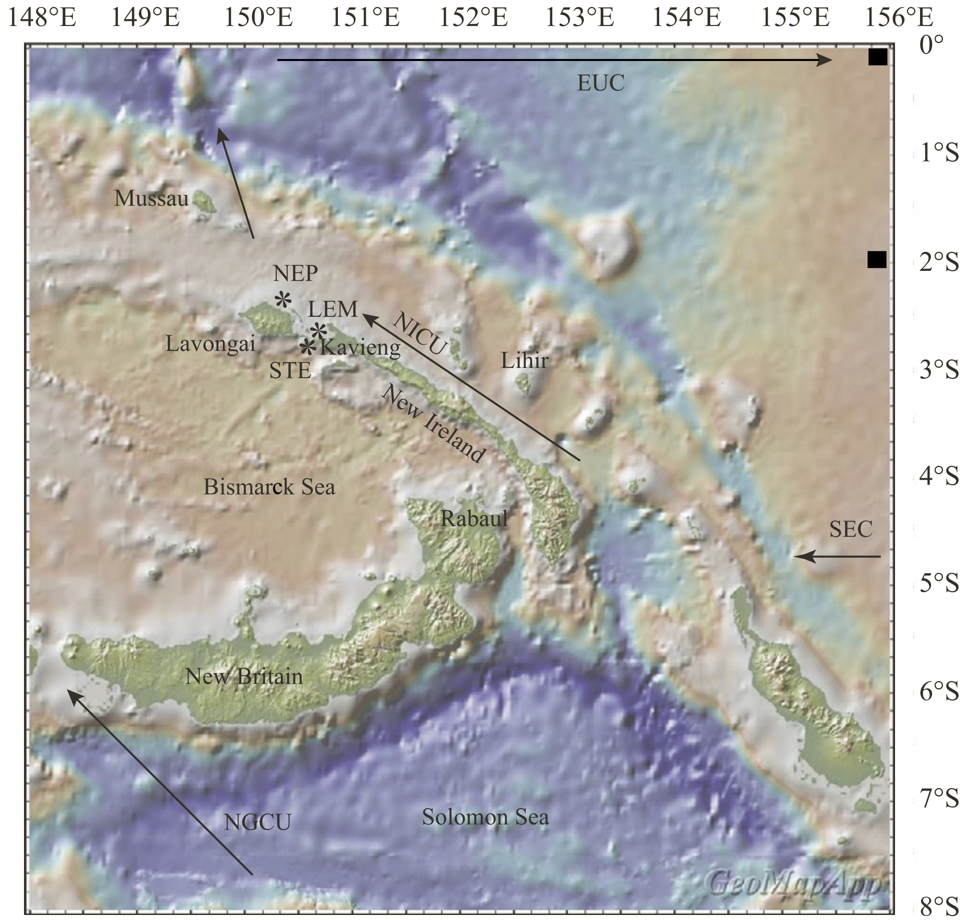

Figure 1. Coral sites near Kavieng, New Ireland: Main coral, northeast pass (NEP), is growing north of Lavongai; Lemus Island (LEM) is growing near Kavieng, and Steffen Strait (STE) is growing at the southern entrance to Steffen Strait. Upper currents discussed here include the South Equatorial Current (SEC), the New Ireland Coastal Undercurrent (NICU), diverted northward by Mussau Island and joining the Equatorial Undercurrent (EUC) at 149°E, and the New Guinea Coastal Undercurrent (NGCU) passing through the Vitiaz Strait. Branches of the SEC can be present anywhere between 0 and 5°S, down to 200 m. Two Tropical Atmosphere-Ocean (TAO) moorings at 156°E are indicated by solid squares. Topographic map was obtained from Marine-Geoscience Data Management System (available at http://www.marine-geo.org) [*Arko et al.*, 2007].

Porites colony 2.10 m high, 3 m wide, growing in 8 m water depth. The three consecutive pieces of this core are coined NEP1, NEP2 and NEP3. The basal section (first ~11 years of growth) was not analyzed.

[5] LA-ICPMS analyses were obtained using a Fisons PQII and a sample stage that holds 100 mm long coral samples. Up to 4 slices per core have been used to optimize sampling along coral growth vectors and provide replicate analyses. The top of NEP1 (main slice) was prepared as 11 contiguous 45 mm long pieces to fit an earlier smaller stage. The top piece was cleaned in an ultrasonic bath with 30% hydrogen peroxide to remove remains of coral tissue. An ArF excimer laser was focused onto the coral surface to a 500 μm by 50 μm rectangle, scanning the coral surface along the growth direction at 2.4 mm/min. The ablated sample was entrained within the stage in a helium gas stream, with Ar being added prior to injection into the ICP. Two preliminary laser scans of the coral were carried out to clean the coral surface and condition the ICPMS cones. The subsequent analytical scan measures the isotopes ^{46}Ca or ^{43}Ca, ^{84}Sr, ^{25}Mg, ^{238}U, ^{11}B, ^{120}Sn and ^{138}Ba, completing a measurement cycle in $^1/_2$ second and using a laser pulse rate of 5 Hz. A further scan, at 10Hz pulse rate, followed for the low-content trace elements, measuring the isotopes Ca^{46}, Ba^{137}, Mn^{55}, Y^{89} and Cd^{111}. Under these conditions, a layer of a few microns of aragonite was removed by each laser scan. Instrument tuning was optimized for Sr, achieving a typical sensitivity of 2×10^5 counts per second on ^{238}U for the NIST 612 glass (with a 50 μm spot, 5 Hz laser pulse rate and 5 J/cm^2 energy density), while keeping ThO$^+$/Th$^+$ ratio below 0.3%. Corrections for drift and calculation of elemental ratios were made by bracketing the coral scan with analyses of a few mm of standard material. Two standards were used. For the elements B, Mg, Ca, Sr, Ba, and U, we used a pressed coral powder containing 10% of acid-cleaned KelF® (teflon beads). The lower-concentration trace elements were standardized against NIST SRM 614. Run quality was monitored using the signal to background ratio and the consistency between Sr/Ca, U/Ca and Mg/Ca ratios, as these three elements are strongly correlated in this coral. The small

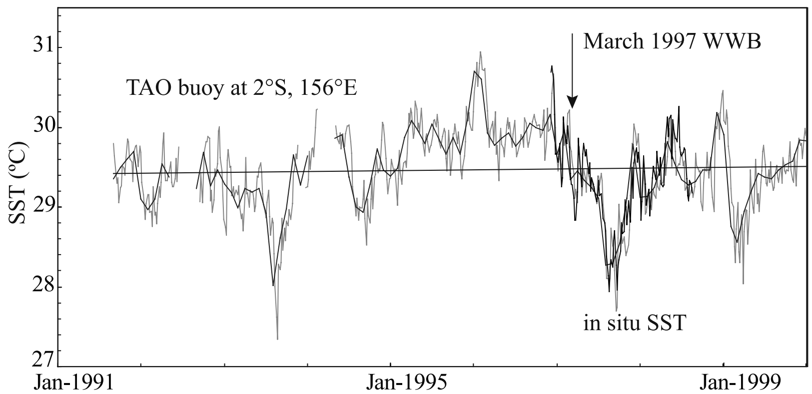

Figure 2. In situ water temperatures at Kavieng harbor, obtained from Frederic Taylor (10 measurements per day) (bold black curve), are in good agreement with sea surface temperatures (SSTs) from the TAO/Triangle Trans-Ocean Buoy Network (TRITON) mooring at 2°S, 156°E (gray curve). Both are shown as 5-d average temperatures. An arrow indicates the very strong westerly wind burst (WWB) between 28 February and 19 March 1997. Thin black curve is a monthly average for the TAO data.

^{46}Ca isotope was measured, as ^{43}Ca was frequently too large to be measured in pulse counting mode, except for the latest analytical sessions. Good runs showed a drift of only a few percent between the bracketing standard analyses and a relative standard deviation (rsd) < 2.5% for Sr/Ca. The errors based on counting statistics, or estimated as residuals between consecutive runs along the same track, are 1–2% for Sr/Ca and Ba/Ca. Including uncertainties associated with possible unaccounted drift effects and the variance of standard measurements, errors around 2% for Sr/Ca and 5% for Ba/Ca are more realistic estimates. The $\frac{1}{2}$ second measurement cycle corresponds to a spatial resolution of 20 μm. Data were averaged to 200 μm resolution, which corresponds to 5–7 d of coral growth. This results in 2σ errors around 1.5% for Sr/Ca and 3.5% for Ba/Ca. Replicate analyses have been made along nearby tracks, or on adjacent slices of the coral core. Ba concentration in the seawater samples was determined by solution ICP-MS. Drift was monitored by addition of an internal standard containing ^{9}Be, ^{115}In, ^{169}Tm and ^{233}U, and a basalt from Kilauea, Hawaii, was used as external standard. The analytical error is ~1%.

[6] SSTs and the depth of the 20°C isotherm were obtained from the Tropical Atmosphere-Ocean (TAO) moorings at 2°S, 156°E and 2°S, 165°E (http://www.pmell.noaa.gov/tao). We also used SSTs from the NOAA analysis at the grid 2.5°S, 150.5°E [*Reynolds et al.*, 2002], available at http://iridl.ldeo.columbia.edu/SOURCES/.IGOSS/.nmc/.Reyn_SmithOIv2., and SSTs from the Hadley Center (HadISST Version 1.1) [*Rayner et al.*, 2003]. Selected grids at the latitude of Kavieng include the merchant-shipping lane along 155°E that has provided reliable data since 1964 [*Morrissey*, 1992]. Subsurface temperatures were obtained from the Simple Ocean Data Assimilation (SODA) reanalysis available back to 1958 (Version 1.4.2) [*Carton et al.*, 2005], and averaged for the grids 2.25°S, 150.25–154.75°E. As indices of ENSO, we used NINO3,4 which is the central east Pacific SST (5°N–5°S, 120°W–170°W), extracted from the HadSST2 data set [*Rayner et al.*, 2005], and Darwin sea level pressure anomalies. A summary and maps of historical tropical cyclones around north Australia, produced by the Australian Bureau of Meteorology, were consulted, as a tropical cyclone developing in the Solomon Sea and tracking southeasterly is a typical synoptic pattern favorable to strong westerlies along the equator [*Vecchi and Harrison*, 1997]. Surface wind data over the domain 0.95–2.86°S, 148.125°E–155.625°E (2° by 2° spatial resolution) were derived from the National Centers for Environmental Prediction (NCEP) ocean analysis [*Kalnay et al.*, 1996]. The zonally averaged wind stress was calculated using a drag coefficient of 1.2×10^{-3} and taking into account the variance of zonal and meridional velocity components, along the lines suggested by *Clarke and Lebedev* [1996]. To assess the hypothesis of horizontal advection of waters from the equatorial region of upwelling west of the dateline, we used the monthly surface current data set from Ants Leetma, available at http://iridl.ldeo.columbia.edu/SOURCES/.IGOSS/.leetma. SeaWIFs images of Chlorophyll a, available since October 1997, were examined using the GES-DISC Interactive Online Visualization And Analysis Infrastructure (Giovanni) from NASA (http://reason.gsfc.nasa.gov/OPS/Giovanni/ocean.seawifs.shtml.)

3. Western Pacific Warm Pool, Upper Currents, and Depth of the Thermocline

[7] The warm pool is characterized by uniform SST around 29°C and weak trade winds, with interannual variations of less than 2°C associated with the El Niño–Southern Oscillation (ENSO). In situ water temperatures measured at Kavieng during the very strong El Niño of 1997/1998 (courtesy of Frederick Taylor), are in good agreement with SSTs from the TAO mooring at 2°S, 156°E, ~700 km further east (Figure 2), validating the use of HadISST for the domain 2.5°S, 150.5–156.5°E to compare with the coral record. The main seasonal cooling in August is enhanced during El Niño. During February–March and September–October the South Equatorial Current (SEC) penetrates further into the western Pacific, enhancing the seasonal cooling [*Reverdin et al.*, 1994; *Johnson et al.*, 2002]. Under La Niña conditions, SSTs remain warm for most of the year, on top of a deep thermocline, and the westward movements

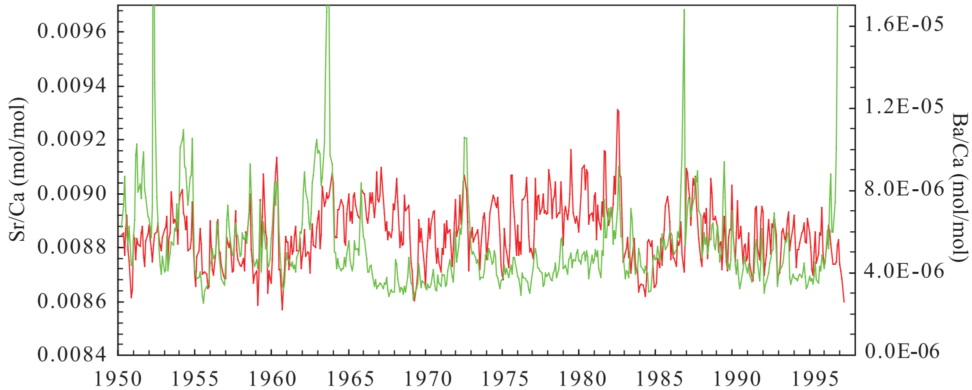

Figure 3. Sr/Ca (red curve) and Ba/Ca (green curve) for the NEP coral, at monthly resolution, back to 1950: Ba/Ca maxima are generally synchronous with Sr/Ca maxima (cool temperature), although the amplitude relationship can vary along the time series. Two Ba/Ca peaks in late 1986 and early 1952, reaching maxima of 3.5 and 2.1 μmol/mol, respectively, are instead associated with warm SST and precede a cooling, as expected after a westerly wind burst.

of the cold tongue (CT) rarely extend beyond 160°E. The reversal of the trade winds between October–April is accompanied by energetic westerly wind bursts (WWBs) typically lasting 5–15 d. As westerly wind anomalies develop in the western Pacific, cyclones forming in the off-equatorial regions raise the thermocline by Ekman pumping and initiate strong southerlies in the Solomon Sea and Coral Sea [*Mayer and Weisberg*, 1998; *Maes et al.*, 1998]. Both surface evaporation and entrainment of cold water from below the thermocline contribute to the temperature cooling of the upper water layer [*Meyer et al.*, 1986; *Liu et al.*, 1994; *Wijesekera and Gregg*, 1996]. Following a WWB in January 1993, a phytoplankton bloom of more than 300 km extent was observed during TOGA-COARE around 156°E [*Siegel et al.*, 1995]. Furthermore, it is expected that owing to the steep bathymetry, northwesterly alongshore winds can induce upwelling to the north of New Ireland.

[8] In contrast to the uniform SSTs, upper ocean currents and subsurface temperatures are remarkably variable. The SEC supplies high-salinity and nutrient-rich waters in the central Pacific and deepens with the thermocline in the western equatorial Pacific. The main contributor to the Equatorial Undercurrent (EUC) is the New Guinea Coastal Undercurrent (NGCU) [*Tsuchiya et al.*, 1989]. *Butt and Lindstrom* [1994] found another undercurrent along the northern coast of New Ireland, connecting to the EUC along 149°E, and named it the New Ireland Coastal Undercurrent (NICU) (Figure 1). According to these authors, the NICU and NGCU are dynamically similar. Direct measurements of the NGCU and EUC at 142°E [*Kuroda*, 2000; *Ueki et al.*, 2003] and of the EUC at 165°E [*Johnson et al.*, 2002] have documented seasonal and interannual variations. During El Niño, both the EUC and the NGCU intensify and shoal, in accord with the reduced zonal slope of the thermocline. While a rise of the 20°C isotherm from 200 m to 150 m is typically observed at the 2°S, 156°E TAO buoy between Niña/Niño events, *Ueki et al.* [2003] reported a shoaling of the core of the NGCU by 100 m during the growing phase of the 1997/1998 El Niño. As also observed for the EUC at 156° E [*Huyer et al.*, 1997], the shoaling of the undercurrent is accompanied by diapycnal conversion (warming).

4. Chronology of Coral Growth for NEP1

[9] Determining the chronology has not been straightforward for the NEP coral due to the complexity of growth revealed by X rays as density banding (Figure S2). Sr/Ca maxima (cold temperature) correspond closely to high-density bands (HDBs) appearing dark on the X-ray positive. In the middle part of NEP1, each broad HDB corresponds to the midwinter minimum temperature, but additional dark bands, for example in the top 140 mm, correspond to semiannual cooling events. Consequently, the spacing between successive HDBs does not always reflect the annual extension rate.

[10] Several considerations were used in establishing the coral chronology. These have included the requirement that the extension rate should be relatively smooth, with significant changes occurring only when also supported by the X-ray image. The identification of annual cycles in the Sr/Ca pattern and their correspondence with SST was generally clearer at times of anomalously cold SST associated with El Niño. Significant Ba/Ca maxima synchronous with some of these events strongly suggest a direct relationship. Thus in selecting tie-points between the coral record and SST, some coupled Ba/Ca and Sr/Ca maxima have been associated with a known El Niño event, provided that, in doing so, the coral extension rate remains sensible. Additional tie-points, taken at seasonal maximum or minimum SST, have been used to accommodate changes of extension rate and improve the fit between Sr/Ca and instrumental SSTs.

[11] Corallite fans are only about 20–25 cm long and their complex geometry has necessitated the use of several adjacent coral slices in order to assemble a continuous record. Replicate Sr/Ca and Ba/Ca analyses (Figure S3) have been averaged to produce a composite record at monthly resolution (Data Set S1 and Figures 3 and S6). Figure 3 highlights

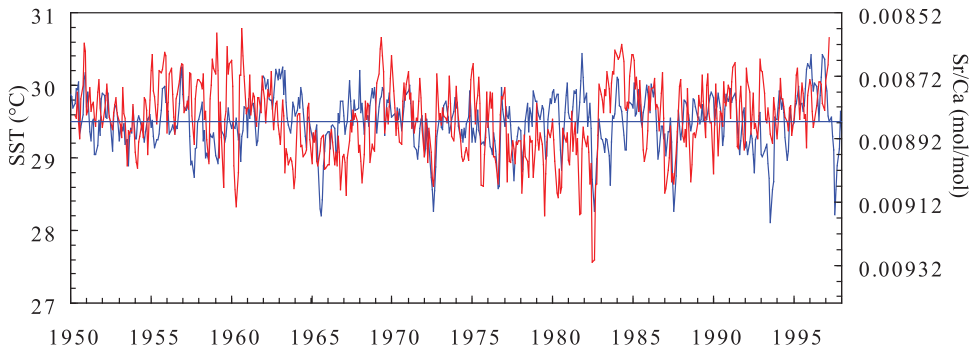

Figure 4. Sr/Ca (red curve) at monthly resolution, back to 1950, is compared with SSTs from HadISST (blue curve) averaged for the grids 2.5°S, 150.5–156.5°E, and detrended relative to a mean temperature of 29.5°C between 1982–2000. Sr/Ca was scaled using a slope of –0.23 mmol/mol per °C and an intercept of –0.01565 mol/mol.

the generally synchronous timing of Ba/Ca and Sr/Ca maxima, despite a highly variable amplitude relationship. Figure 4 shows monthly Sr/Ca compared with instrumental SSTs.

[12] The strong El Niño events of 1972, 1982, and 1987, characterized by anomalously cold SST for most of the year (Figure 4), were identified in the coral by a marked Sr/Ca maximum. The tie-point taken in November 1986 to account

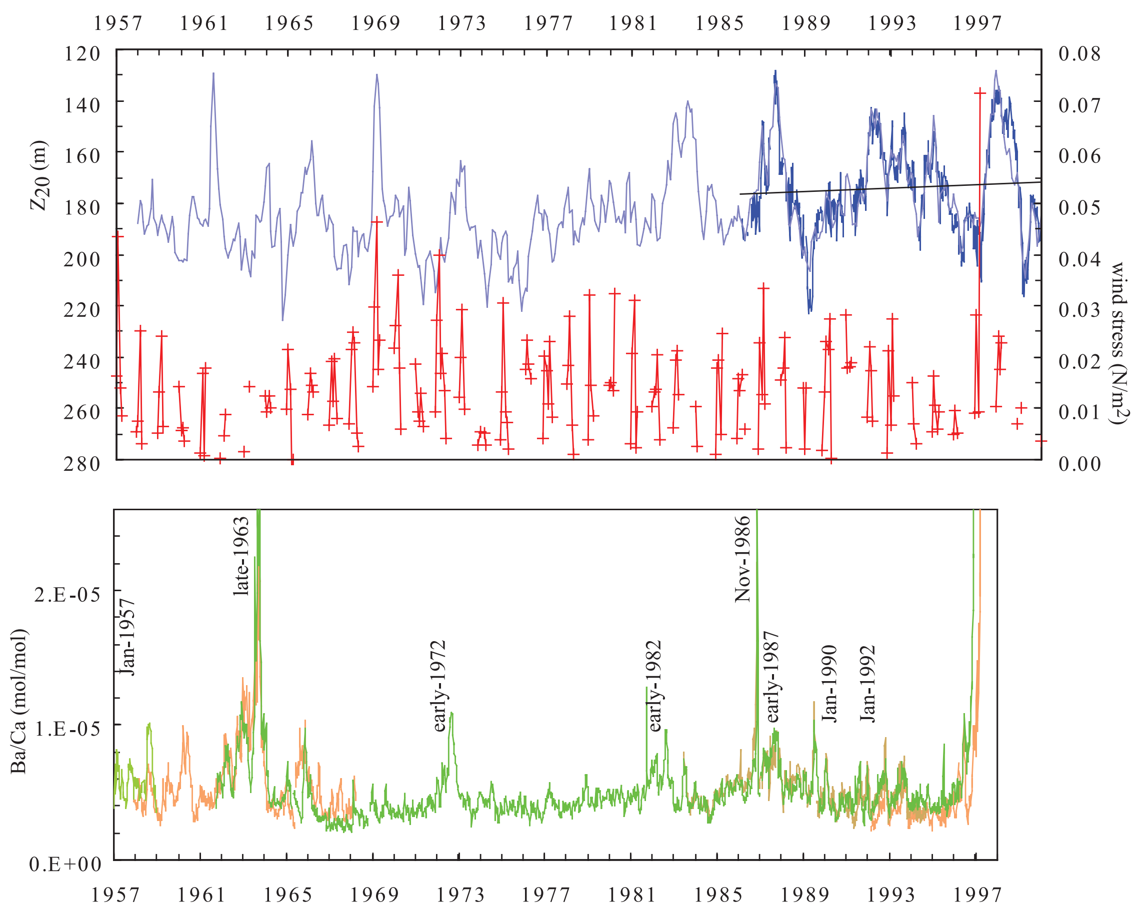

Figure 5. Northwesterly component of the wind stress (National Centers for Environmental Prediction (NCEP)) (red curve), averaged over the domain 0.95–2.86°S, 149.125°E–155.625°E, is compared with the depth of the 20°C isotherm (Z_{20}) at 2°S between 150–155°E (Simple Ocean Data Assimilation (SODA) reanalysis, pale blue curve). Both data sets are monthly means. Z_{20} data from the TAO/TRITON buoys at 2°S, 156°E and 2°S, 165°E were blended as weekly average (darker blue curve) and show the very rapid response of the upper ocean to WWBs. Favorable conditions for upwelling along the northern coast of New Ireland occur when anomalous westerlies or alongshore northwesterlies ($\tau > 0.02$ Pa) are associated with rising or shallow thermocline. Ba spikes and small peaks attributed to WWBs are labeled.

for a major change of extension rate corresponds to a Sr/Ca minimum synchronous with a very large Ba spike. These may trace the strong WWBs of late 1986 [*Vecchi and Harrison*, 1997] leading to the rapid rise of the thermocline by January 1987 (Figure 5). Between 1987 and the top of the coral, the extension rate remains high, at ~17 mm/a (Figure S3). Two additional tie-points in August 1993 and February 1996 have been taken to optimize the fit to SSTs. During the prolonged and unusual El Niño 1991–1993, moderate Ba peaks are observed in the coral, consistent with a very shallow thermocline (Figure 5) [*Kessler and McPhaden*, 1995]. Two narrow Ba peaks dated as early 1992 and early 1990 may trace the WWBs of January 1992 and February–March 1990, respectively [*Cronin and McPhaden*, 1997; *Kuroda and McPhaden*, 1993; *Vecchi and Harrison*, 1997]. Additional tie-points in 1983, 1980, and 1976, characterized by clear Sr/Ca maxima, account for minor changes of extension rate. There is no Ba signal associated with the weak El Niño in 1976/1977, suggesting that the local thermocline remained too deep, in agreement with the SODA reanalysis (Figure 5). Relatively uniform SSTs during the years 1977 and 1978 are associated with a single broad and diffuse HDB on the coral X-ray image (Figure S2).

[13] Prior to 1968, dating was more difficult due to multiple changes of direction of the corallite fans, reflected by diffuse and complex HDBs, and skeleton fissures around the mid-1960s and 1954. The two El Niño events of 1965/1966 and 1957/1958 are not clear in the coral record. A tie-point was taken in 1969 along the central axis. May 1965 and August 1957 were used as distinctive markers in the side sections to determine the fine chronology further down. A large and reproducible Ba/Ca cluster is dated as 1963, rather than being associated with El Niño 1965/1966. This peak includes successive spikes > 20 μmol/mol which correspond to thin dark bands on the X-ray positive. These are rather suggestive of WWBs and consistent with anomalous westerlies during the second half of 1963 between 140°E and the dateline [*Wang*, 1995] and wind records from islands near the dateline [*Harrison and Giese*, 1991]. Near the base of NEP1, another large Ba/Ca spike (52 μmol/mol) occurs during El Niño 1951/1952. It could be related to local upwelling triggered by westerlies associated with tropical cyclone "TC 0225", which intensified in the Solomon Sea in April 1952 and was the strongest reported in that region between 1950 and 1965. Taking August 1952 and August 1957 as tie-points accounts for the apparent high extension around 1955. Small to moderate Ba peaks between 1957 and 1959 match the prolonged El Niño conditions suggested by persistent anomalous westerlies north of New Guinea [*Wang*, 1995]. The year 1957 appears as a distinctive dark band on the X-ray positive (Figure S2).

[14] Overall, the uncertainty in the timing of seasonal features, e.g., Sr/Ca-derived temperature maxima or minima, is estimated to be up to about 3 months. For example, the period 1960–1963 could possibly be shifted later by 3 months to better match the December 1963 WWBs. While the identification of most tie-points is considered to be robust, the complexity apparent in this coral makes it possible that discrete errors of ±1 year have been introduced in the dates attributed to some tie-points, particularly in the older parts of the coral core, for which comparative reconstructed data may be less reliable (see part 2, *Alibert and Kinsley* [2008]). The base of this first length of the NEP coral is therefore dated as 1950 ± 1 year.

5. Sr/Ca-Temperature Relationship and "Vital Effects"

5.1. Calibration of Sr/Ca Against Instrumental SST

[15] Replicate analyses along nearby tracks (Figure S3) are generally consistent with each other, except when the laser track is badly aligned with the coral growth axis, in which case Sr/Ca patterns can appear significantly distorted and poorly reproducible, as for example during the 1960s, the 1930s (Figure S4), the 1860s, or between 1881 and 1884 (Figure S5). Duplicate LA-ICPMS analyses along the same track show a high degree of reproducibility of even the fine detail of trace element patterns, which indicates that the large amplitude variations of Sr/Ca are not the result of analytical noise.

[16] Figure 6a compares several published Sr/Ca-temperature relationships obtained from high-precision TIMS, high-resolution ICPMS or ion microprobe. Whenever possible, these data have been normalized to the mean Sr/Ca = 0.008509 (± 2 E-06 standard deviation) obtained for seawater samples collected around Kavieng. Differences between these calibrations are larger than can be expected from analytical accuracy (0.2–1°C), seasonal variations of the growth rate [*Cardinal et al.*, 2001], or variations in

Figure 6. (a) Previously reported Sr/Ca-temperature calibrations derived from high-precision thermal ionization mass spectrometry (TIMS), multicollector inductively coupled plasma mass spectrometry (ICPMS) or ion microprobe (secondary ion mass spectrometer (SIMS)). Data points for the NEP coral cover the period 1950–1997. Calibration line in bold black (slope of –0.23 mmol/mol per °C and intercept of 0.0156 mol/mol) is not a least squares regression line and was determined as described in the text. Two dashed lines labeled 1 and 2 are for inorganic aragonite precipitation, 1 for *Kinsman and Holland* [1969] and 2 for *Dietzel et al.* [2004]. Other calibrations are for *Porites* corals, unless specified: *Alibert and McCulloch* [1997] for Davies 2 and *Alibert et al.* [2003] for Pandora 1998 (Great Barrier Reef); *de Villiers et al.* [1995] for Koko-2 (Hawaii); *Beck et al.* [1992] and *Quinn and Sampson* [2002] for New Caledonia; *Evans et al.* [1999] for Kiritimati; *Wischow* [1999] for La Reunion, Abrolhos Island, and Ningaloo Reef (west Australia); *Marshall and McCulloch* [2001] for Christmas 8 (Christmas Island); *Felis et al.* [2004] for Eliat-15B (Red Sea); *Swart et al.* [2002] for a *Montastraea* coral from Florida; *Cardinal et al.* [2001] for two *Diploria* corals from Bermuda; and *Allison and Finch* [2004] for Hawaii (SIMS). Calibration parameters have been normalized to the Kavieng seawater composition for corals from Davies and Pandora Reefs (reported Sr/Ca = 0.008484), La Réunion (Sr/Ca = 0.008571), Abrolhos Island (Sr/Ca = 0.00858), and Ningaloo Reef (Sr/Ca = 0.008571). (b) Slope and intercept parameters for the calibrations plotted above (same symbols), after a normalization to the mean temperature at each coral reef location. Two data points labeled NEP are for laser ablation (LA)-ICPMS and TIMS analyses.

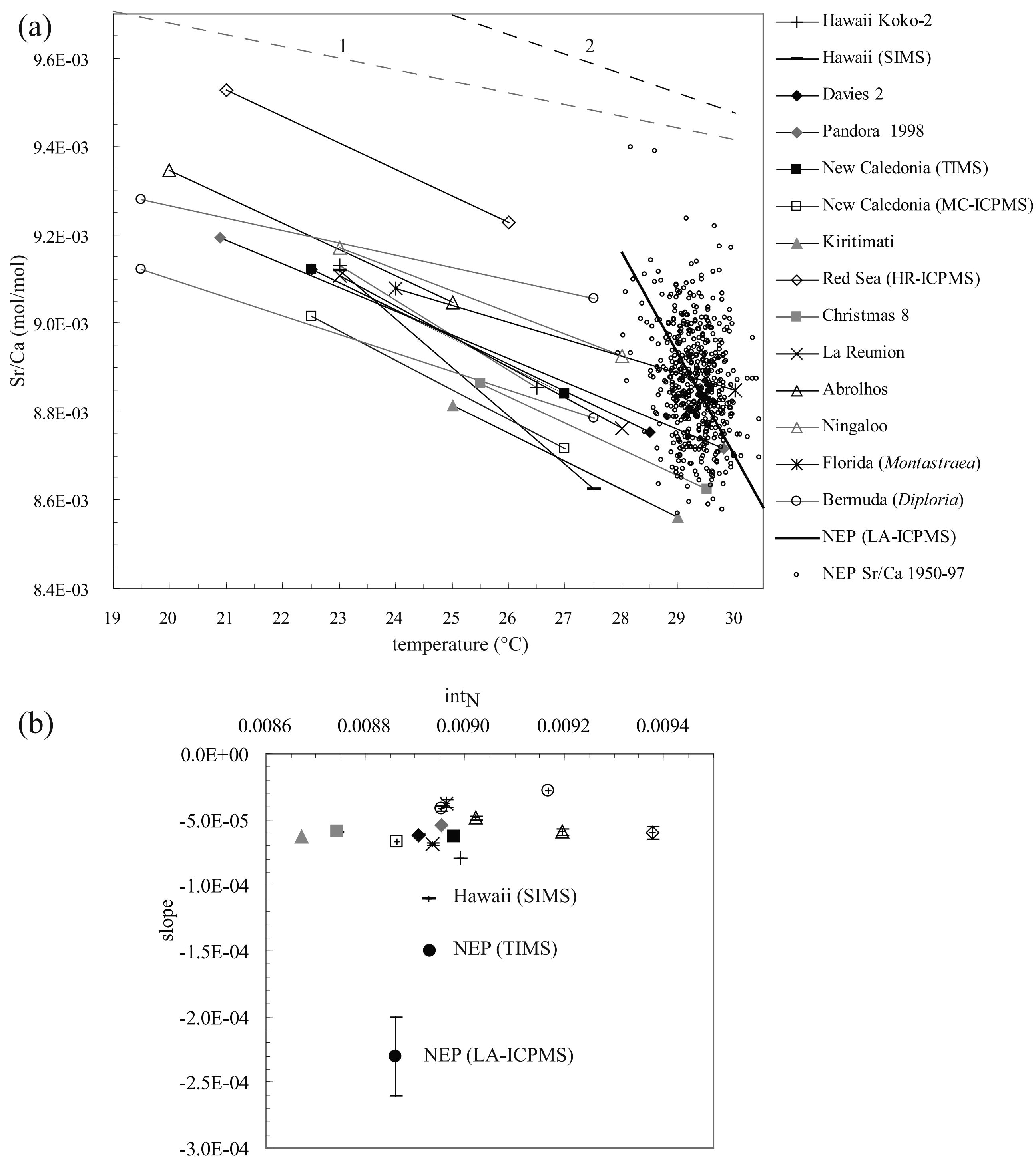

Figure 6

seawater composition associated with upwelling (~2%) [*de Villiers*, 1999]. The Sr/Ca data points for the NEP coral cover a large range of Sr/Ca for a SST range of only 1–2°C, and are clearly not in accord with other coral calibrations showing a weaker slope around −0.06 mmol/mol per °C. Part of the scatter in the NEP data can be attributed to greater error bars for LA-ICPMS analyses than would be the case for TIMS. At monthly resolution, the LA-ICPMS data have approximately 1% error in the Sr/Ca ratio, whereas TIMS-based data would be a factor of 4 more precise. The large spread shown by the data indicates that factors other than temperature alone affect the Sr/Ca ratio in this coral. Over such a small temperature range, a least squares regression line is poorly defined, with large errors in the slope and intercept. Also, if other parameters are involved, a simple regression is not likely to be meaningful. As an alternative calibration technique, we have attempted to match the amplitude of the Sr/Ca and SST variations during the El Niño years, such as 1987, 1982, and 1972. These represent the largest SST variations in the warm pool, so the temperature dependency

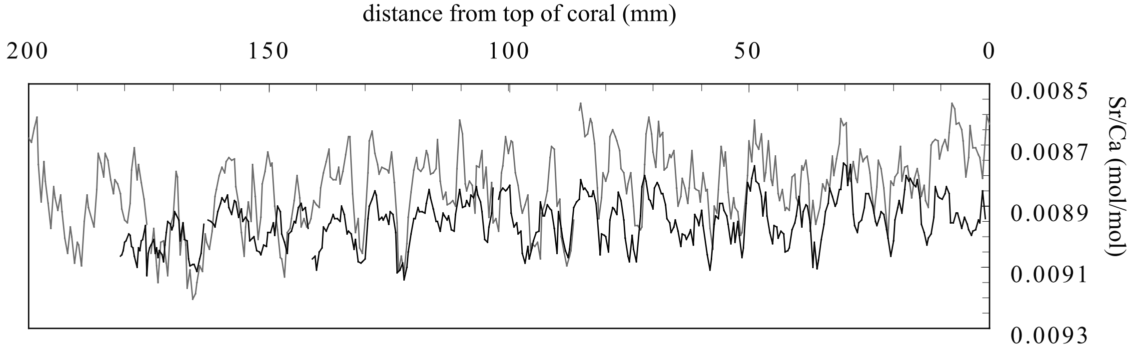

Figure 7. Sr/Ca measured by ICPMS (gray curve) along track "c" (see Figure S2) is compared with TIMS data (black curve) obtained along track "a" for the top 20 cm of NEP1. ICPMS data have been averaged to the same spatial resolution of 0.5 mm used for the TIMS sampling, equivalent to 10–15 d of linear growth.

of the Sr/Ca ratio should be at its greatest. This establishes the slope or sensitivity of Sr/Ca to temperature. The intercept is then determined by matching the long-term mean Sr/Ca (0.00886) to the mean SST (29.3°C) between 1950 and 1998. The standard deviation of the residuals between calculated and instrumental temperature remains within ±0.5°C. The resulting calibration has a slope of –0.23 mmol/mol per °C and an intercept of 0.0156 mol/mol. As SSTs show a long-term upward trend (Figure S6), the mean Sr/Ca-derived temperature is slightly shifted up relative to SSTs prior to 1950. Nonetheless, in extending this calibration method to the full coral record, the sensitivity to temperature remains similar back to 1870, at –0.23 ± 0.03 mmol/mol per °C.

[17] Sr/Ca variations obtained by ICPMS and TIMS (Figure 7) show consistent patterns, but the TIMS analyses show smaller amplitude variations and a shift to higher ratios. The laser track was 1.5 cm away from the TIMS transect. A much larger volume of coral powder is sampled for TIMS analysis and beyond ~140 mm (around 1986), the sampling transect is at a significant angle from the growth vector, which may both contribute to the reduced amplitude. The Sr/Ca obtained by TIMS, compared with SSTs at a similar 15-d resolution (IGOSS/Reynolds) gives a slope around –0.17 mmol/mol per °C and an intercept of 0.014 mol/mol.

[18] A plot of slope versus intercept for the calibration lines in Figure 6a would show an apparent alignment caused by the fact that the intercept at 0°C is far away from the temperature of the coral environment. We have instead normalized the temperature range to the mean temperature at each reef location. This results in the normalized intercept being equal to the mean Sr/Ca ($int_N = Sr/Ca_m$) in Figure 6b. The calibration slopes appear independent of the mean Sr/Ca at each location. Importantly, the normalized intercept value for the NEP coral, hence long-term mean Sr/Ca value, is not anomalous compared to the other calibrations.

5.2. Sampling Resolution

[19] Sampling resolution is the most straightforward origin for at least part of the large amplitude of the Sr/Ca signal in the NEP coral, as the sampling size between laser ablation and TIMS is vastly different. Sampling at high spatial resolution highlights details of the Sr/Ca signal, including possible heterogeneities of composition dependent on the fine-scale architecture of the skeleton. Most of the calibrations shown in Figure 6a have been obtained using a similar method (sampling with a microdrill at near-monthly resolution along the growth vector), but in order to collect 1–3 mm^3 of coral powder, the sampling in the other two dimensions is significantly greater. This is likely to produce more smoothing of the Sr/Ca signal than anticipated. By contrast, ion microprobe measurements at subdaily resolution [*Allison and Finch*, 2004] give a stronger slope of –0.11 mmol/mol per °C (monthly data, see Figure 6b). These authors show that the degree of data smoothing has a large impact on the slope, which changes from –0.13 mmol/mol per °C for daily data, to –0.08 mmol/mol per °C when a 77-d running mean is applied. When a similar smoothing is applied to the NEP LA-ICPMS data, the slope is in accord with that indicated by our TIMS data, which however still represents a higher sensitivity of Sr/Ca to temperature than is observed for other corals. The calibration for the Rabaul coral [*Quinn et al.*, 2006] is similar to that observed for other *Porites* corals, even though SSTs are comparable to those around Kavieng, except for slightly cooler winters during the El Niño events. The sampling size indicated is a few cubic millimeters, again 3 to 4 orders of magnitude greater than for laser ablation, so it would be much less sensitive to fine-scale structure in the Sr/Ca signal. In the Rabaul coral, Sr/Ca maxima during the El Niños of 1972, 1982, 1987, and 1993, characterized by similar SST minima, vary by more than 0.5% (compared to a total seasonal range of 2%), suggestive of a variable response to temperature. This is also observed in the NEP coral, with additional apparent shifts of Sr/Ca relative to temperature, e.g., from 1978 to 1982, which are difficult to explain. Together, these observations suggest that the response of Sr/Ca to temperature may be variable over time and that other factors have a significant influence on Sr/Ca.

5.3. Kinetic or Biological Controls?

[20] *Plummer and Busenberg* [1987] showed that Sr uptake by aragonite in thermodynamic equilibrium with seawater gives a $K_d \approx 10$ at 25°C, while experimental inorganic precipitation gives K_d' slightly above 1 [*Kinsman and Holland*, 1969; *Dietzel et al.*, 2004], which is closer to values measured in corals. This deviation from thermodynamic equilibrium has been explained by the high precipitation rate relative to diffusion rate of Sr in aragonite, and

ascribed to surface-dependent kinetics, with K_d' depending on the ion coordination number [*Kinsman and Holland*, 1969]. Although this kinetic control has since been studied mainly in calcite [e.g., *Tesoriero and Pankow*, 1996], the general predictions remain valid for aragonite: high growth rates lead to increased K_d' for elements with $K_d' < 1$ and decreased K_d' for elements with $K_d' > 1$ [*Watson*, 2004]. In consequence, a surface kinetic effect predicts that K_d' for Sr, Ba and U, which are slightly above 1 in aragonite, will tend to decrease with increasing calcification rate.

[21] Such kinetic effects may explain high Sr/Ca and Ba/Ca ratios measured when transects approach a margin between two adjacent fans of corallites, where the coral skeleton shows low-density and slow extension rate, hence also calcification rate. This is observed for part of one analysis track covering the period 1927–1930 (green track in Figure S4). On the other hand, two parallel growth axes with different extension rate between 1911 and 1917 do not show different mean Sr/Ca, and the rapid increase of extension rate after 1987 does not affect Sr/Ca in a clear way. Therefore kinetic effects cannot be readily inferred from the extension rate alone.

[22] As the duration of the cooling indicated by Sr/Ca during the El Niño winters matches closely that indicated by SST (Figure 4), there is little evidence to suggest that the extension rate varies significantly during the year. In consequence, variations of calcification rate may mirror instead those of the skeletal density. We propose that variations of the calcification rate contribute to the distinctly stronger temperature sensitivity of the NEP coral, with a relatively lower calcification rate during the warmer periods and higher rate during the cooler periods. The latter are generally associated with the shoaling of the NICU (August–October), WWB-triggered coastal upwelling or the penetration of the SEC in the western equatorial Pacific during strong La Niña events. The inferred higher calcification in the NEP coral in winter does not appear to be stress related. On the contrary, HDBs formed during periods of below average SST point to more optimal calcification conditions. Increased tissue layer thickness, hence also coral health, has been shown to be associated with the formation of HDBs [*Cruz-Piñón et al.*, 2003]. *Helmle et al.* [2000] used X-ray computed tomography to demonstrate that HDBs correspond to thickened specific structures of the coral skeleton, such as septa. This thickening could coincide with the optimum temperature for calcification. Long-term experiments in the Great Barrier Reef (GBR), measuring the calcification rate under natural temperature conditions, have led *Marshall and Clode* [2004] to determine an optimum at ~25°C, clearly below the average summer SST of 28°C. This is consistent with the formation of HDBs generally in early summer for *Porites* corals from GBR [*Lough and Barnes*, 1990], but it is probable that the combination of favorable environmental conditions is not universal. Around New Ireland, this optimum may instead occur during the cooler months. Although the effect of nutrients on calcification is not yet well understood, beneficial effects on coral growth rate, tissue proteins and rate of photosynthesis have been reported after 5 weeks of zooplankton feeding [*Houlbrèque et al.*, 2003; *Ferrier-Pagès et al.*, 2003].

[23] A major issue remains though, which is how the Sr/Ca distribution coefficient between coralline aragonite and seawater responds to changes of the calcification rate. The positive correlation between Sr/Ca and calcification rate inferred for the NEP coral may reflect a biological control rather than crystal surface effects. Recent biological studies [*Allemand et al.*, 1998; *Cuif and Dauphin*, 2005] have shown the role of the organic matrix in the regulation of coral calcification. A temperature-related change in activity of the transport enzymes could also occur, as an adaptation to high SSTs, as previously proposed by *Clausen and Roth* [1975] for other equatorial corals. *Rickaby et al.* [2002] proposed a mechanism to account for rate-dependent Sr/Ca ratios in the coccoliths of *E. huxleyi.* It is based on selectivity against Sr and other ions with a larger effective ionic radius than Ca^{2+}, during the transport of Sr^{2+} and Ca^{2+} via ion channels or carrier proteins. A reduction of selectivity at high pumping rate would lead to increased Sr/Ca in the calcifying fluid. The high K_d' values for Sr, U and Mg in the NEP coral, despite differences in ionic radius between these three elements, appear consistent with such a mechanism.

[24] The NEP coral, with its unusual Sr/Ca record, likely represents an extreme member of a range, where Sr/Ca is dominated by biological controls rather than temperature. It is likely that similar biological effects are present to varying degrees in all coral Sr/Ca records. While most published calibrations for modern *Porites* corals are broadly similar, paleo-SSTs derived from coral Sr/Ca alone must be viewed with caution.

6. Ba/Ca Variations in the NEP Coral and Their Significance

[25] Major Ba/Ca peaks around 7–10 μmol/mol occur in austral winter, during the growing phase of El Niño. Prior to 1950, their amplitude can be up to 20 μmol/mol (Figure S6). The background Ba/Ca, around 4 μmol/mol, is similar to that measured in *Porites* corals from GBR [*Alibert et al.*, 2003; *Fallon et al.*, 2003] or New Caledonia [*Quinn and Sampson*, 2002] and corresponds to the uptake of dissolved Ba from ambient surface seawater, with a distribution coefficient close to 1 [*Lea et al.*, 1989]. The Kavieng seawater Ba concentration is 35 nmol/kg, similar to that obtained for surface waters from midreef GBR [*Alibert et al.*, 2003]. The transient Ba spikes between 10–50 μmol/mol, which usually precede a sharp fall of SST, such as in late 1986, late 1963, or early 1952 (Figure S3), appear to be linked to upwelling triggered by strong WWBs. The Ba enrichment observed in the NEP coral is markedly higher than previously reported in corals growing away from riverine influence [*Lea et al.*, 1989; *Tudhope et al.*, 1996]. The latter authors reported Ba/Ca peaks in corals from Oman, during the upwelling season, at 2–3 times the background level. The NEP Ba/Ca peaks also exceed those reported for corals growing in the path of river flood plumes off the North Queensland coast [*McCulloch et al.*, 2003], the latter being of the order of 10 μmol/mol during the strongest floods. A terrestrial origin for the Ba enrichment is improbable because of the small size of the New Ireland and Lavongai islands (New Ireland is only 10 km wide). This is also indicated by low manganese and yttrium concentrations, which are two elements highly sensitive to continental influence. The mean Mn/Ca ratio, for the top 40 cm of the core, is

0.136 ± 0.0056 μmol/mol, (equivalent to 75 ppb Mn) and shows small seasonal variations better correlated with Sr/Ca, hence temperature, than with Ba/Ca. The Y/Ca ratio, in the range 20–40 nmol/mol all along the NEP core (equivalent to 20–35 ppb Y), does not show significant variations and is only rarely correlated with Ba/Ca. The closest significant terrestrial source would be the Sepik-Ramu river system north of PNG (at 144°E) with a peak discharge in March–April and lowest discharge in August, in particular during the El Niño drought years. This is inconsistent with the large Ba peaks in the NEP coral synchronous with SST minima (Figure S6). Furthermore, the plumes are usually deflected alongshore by the New Guinea Coastal Current toward the southeast or northwest [*Cresswell*, 2000; *Kineke et al.*, 2000; *Mackey et al.*, 2002]. Dispersion of Ba by horizontal advection across the Bismarck Sea, either as dissolved Ba or as fine particles, is unlikely to reach Kavieng, 700 km to the NE of the Sepik mouth.

[26] The source of the Ba enrichment in the NEP coral is probably thermocline waters from the NICU during wind-driven upwelling or winter shoaling episodes, both favored by the steep bathymetry along the northern coast of New Ireland. In August 1997, an upwelling plume was observed on the southwest New Britain coast [*Cresswell*, 2000], forced by strong southeasterly winds. During the recent weaker El Niño of 2002/2003, SeaWIFs images for October 2002 reveal high Chlorophyll a (~2.5 mg/m^3) along southwest New Britain. Another Chlorophyll-rich spot can be seen north of Lavongai, hence close to the NEP coral, where anomalously strong westerlies along the equator (TAO/Triangle Trans-Ocean Buoy Network (TRITON) winds) may have triggered some coastal upwelling.

[27] Any signature of upwelling in the corals north of New Ireland is likely to depend not only on the intensity of the WWBs, but also on the depth of the thermocline. The amount of nutrients brought up to the euphotic zone will be dependent on the efficiency of the turbulent vertical mixing to erode the stratification at the bottom of the mixed layer. Observations over the COARE domain (between Kavieng and the equator at 156°E) between November 1992 and February 1993, have shown that both thermal and haline stratifications were weakened during WWBs [*Huyer et al.*, 1997]. Figure 5 shows coral Ba/Ca against the depth of the 20°C isotherm, usually taken as an index for the thermocline depth, and the northwesterly (alongshore) component of the wind stress, back to 1958. Some of the small Ba/Ca peaks either isolated (around January 1992) or preceding a winter Ba peak (1972, 1982, or 1987) are typically around 6–7 μmol/mol and correspond to high wind stress (> 0.02 N/m^2) and reported WWBs [*Harrison and Giese*, 1991; *Hartten*, 1996]. The Ba spikes observed in 1986 and 1963 are of much larger amplitude (25 μmol/mol) and followed by a Sr/Ca-derived cooling of ~1.5°C which is larger than the 0.5°C cooling indicated by monthly SSTs (Figure 4), although a 1°C cooling was recorded at the TAO buoy at 2°S, 165°E, following the strong WWB of December 1986. *Maes et al.* [1998] analyzed the heat balance in the COARE domain and found that vertical advection and entrainment had a large contribution to this cooling, compared with the following WWB events of late 1987. Although the coral-derived temperature may be affected by vital effects, the large Ba enrichment supports a strong upward transport and vertical mixing above the undercurrent.

[28] In the warm pool between 150–156°E, the well-documented El Niños of 1982/1983, 1987, and 1993 are characterized by similar SST minima around 28°C, relatively shallow 20°C isotherm depth (130–140 m, see Figure 5) and high wind stress (NCEP winds). The winter Ba/Ca peaks associated with these events are higher for 1982 and 1987 than for 1992–1993 and the 1972 peak slightly larger than that found for 1982. These subtle variations indicate that the amplitude of the Ba/Ca peaks does not depend on the depth of the thermocline alone, but probably also on more local conditions affecting vertical mixing. In the absence of chemical and oceanographic measurements in the NICU, coral Ba/Ca therefore can only be regarded as a qualitative indicator of vertical mixing or biological productivity in this region of the warm pool.

[29] Additional sources of Ba are still necessary to account for Ba/Ca peaks found during other years. We propose a current-driven horizontal advection of nutrient-rich waters to explain these. A Ba peak around June 1983, associated with a shallow thermocline (Figure 5), may not be sourced from the undercurrent. During the very strong El Nino 1997/1998, which showed a similar onset and development to the 1982/1983 event, *Ueki et al.* [2003] reported a shoaling of the NGCU, north of New Guinea, only between July 1997 and February 1998. In early 1998, anomalously strong northeasterlies west of the dateline forced equatorial upwelling [*McPhaden*, 1999; *Grodsky and Carton*, 2001]. Large-scale phytoplankton blooms were reported in April 1998 around 170°E [*Ryan et al.*, 2002] and a weaker signal was detected earlier further west [*Murtugudde et al.*, 1999]. In a similar way, strong northeasterlies along the equator occurred between January and April 1983 (NCEP reanalysis). In consequence, the coral Ba peak of 1983 may trace nutrient-rich waters advected by intensified surface currents in the band eq-2°S.

[30] Other noticeable Ba peaks occur during La Niña, for example in 1996, 1989, 1962, 1954, and 1956, and appear more frequent before 1950 (see part 2, *Alibert and Kinsley* [2008]). High Ba levels in the top 10 mm are due to remains of coral tissue, 6 mm thick at the time of sampling. The Ba peak in May 1996 coincides with the first HDB. During a transect along 150°E, between July and October 1996, at the end of La Niña, *Ioualalen et al.* [2000] reported high-salinity waters between the equator and 2°S, with a core (salinity > 35.5) at 150–200 m, at the depth of the SEC. As these authors noted a westward near-surface zonal flow but no equatorial upwelling or divergent flow, they proposed that the 150°E high-salinity waters originated from the subduction of cold tongue waters at the salinity front around 160°E, by horizontal advective processes. As the high-salinity waters extended to the surface through the Barrier Layer, although diluted, this suggests that nutrients could also have been mixed up to the surface. These nutrients would originate by equatorial upwelling in the more eutrophic regions of the western Pacific, east of 160°E, where nutrient enrichment has indeed been documented [*Radenac and Rodier*, 1996].

[31] The Ba/Ca peak in mid-1989 coincides with the end of the 1988/1989 La Niña. A strong westward surface current was observed between New Ireland and the equator,

between 150°E and 160°E (IGOSS/Leetmaa currents [see also *Frankignoul et al.*, 1996, Figure 4]), well after the seasonal maximum of the SEC. Instrumental SSTs (Figure 4) show that the annual minimum SST around 150°E occurred in April, coincident with the maximum extension westward of the CT [*Picaut and Delcroix*, 1995; *Kuroda and McPhaden*, 1993]. Winds during mid-1975 (NCEP reanalysis), at the end of the strong 1973–1975 La Niña, might lead one to expect a similar Ba peak, however, none is seen in the coral record. During the strong La Niña of 1954–1956, the coral shows an irregular Ba peak in 1954, and a smaller one in 1956 (Figure S3). A marked cooling and smaller Ba peak in early 1960 may also trace nutrients carried along a stronger than normal SEC [*Wyrtki*, 1974], in accord with anomalously strong easterlies in the central Pacific [*Wang*, 1995].

[32] Dissolved barium concentrations in the NICU have not yet been reported but data from various parts of the Pacific and Indian Oceans [*Bacon and Edmond*, 1972; *Chan et al.*, 1977; *Jeandel et al.*, 1996; *Esser and Volpe*, 2002] give a range 35–80 nmol/kg at 0–300 m depth. This is well below the enrichment factor necessary to explain the largest Ba peaks measured in the NEP coral. Nutrients reaching the coral reefs north of New Ireland need not necessarily be in the form of dissolved inorganic nutrients. They could instead be derived from the slow degradation of marine aggregates in the euphotic zone through the bacterial loop. Ba could also be incorporated into the coral as a particulate phase, being trapped and dissolved by coral mucus [*Goldberg*, 2002]. Particulate biogenic barium is often found at the same depth as the deep chlorophyll maximum (DCM) [*Jeandel et al.*, 2000]. Biological productivity increases in the warm pool during El Niño, because of the relatively shallow thermocline/nutricline [*Mackey et al.*, 1997; *Turk et al.*, 2001]. *Mackey et al.* [1997] reporting on a transect along 155°E, between 0–5°S, during 1992 and 1993, found a shallow DCM near the top of the thermocline at 27–28°C. Nutrients from this reservoir could be available to shallow reefs north of New Ireland. Some labile Ba could also be associated with marine snow [*Alldredge and Silver*, 1988], in the form of amorphous barium sulfate, or adsorbed on Fe-oxides associated with phytoplankton surfaces [*Sternberg et al.*, 2005]. *Gorsky et al.* [2003] observed high concentrations of marine snow in the top 50 m of the SEC in late 1996. Marine snow was concentrated along frontal regions and these authors inferred a long survival time before sinking or consumption. This would allow for transport of the smaller aggregates along the SEC over substantial distances and their likely accumulation at the salinity front at the eastern edge of the warm pool.

7. Conclusion

[33] Coral analysis using high-resolution LA-ICPMS captures fine-scale detail in the trace element record that would be difficult to document by more conventional "bulk" analysis techniques. In contrast to previously published coral studies, the NEP coral does not show a simple relationship between Sr/Ca and SST. Nevertheless, we have attempted to utilize the periods of greatest SST variation to extract a best estimate for a temperature response. This "calibration", even with its unusually large temperature sensitivity, still does not account for the full range of Sr/Ca variations observed in this coral, indicating that Sr/Ca is sensitive to other factors, probably also affecting the coral calcification rate. As a result, the utility of the NEP Sr/Ca as a proxy for SST is limited and decadal-scale variations of the order of ±0.5°C are within error margins. We have therefore mainly used the annual SST cycle, generally clear in the Sr/Ca record, as an aid in establishing the coral chronology.

[34] Transient enrichments in Ba during El Niño events are linked to the shoaling of the New Ireland Coastal Undercurrent and occasional coastal upwelling triggered by WWBs. These data reveal an unsuspected role for upwelling along the steep northern coast of New Ireland, entailing an efficient vertical mixing between shallow waters and deeper thermocline waters. Biologically sourced barium may contribute to the high concentrations found in this coral, suggesting that the incorporation of Ba in the coral skeleton is not as well understood as previously thought. Further oceanographic data for the NICU, including depth profiles of Ba and other trace metals, would clarify the sources and transport mechanisms of these elements into the New Ireland surface waters. Controlled experiments are also needed to investigate and quantify the biological mediation of trace element uptake during coral calcification.

[35] In the companion paper for this coral study, we examine the entire coral record back to the early 1820s. Observed decadal to multidecadal changes of magnitude of the Ba/Ca peaks are placed in the context of the climatic changes that have occurred during the last ~170 years, and may have affected the dynamics of the New Ireland Coastal Undercurrent and in consequence the biological productivity in the New Ireland region.

[36] **Acknowledgments.** We thank Malcolm McCulloch for his support and access to analytical facilities at RSES and Graham Mortimer for invaluable help in the laboratory. Fieldwork and research for C. A. were funded by an ARC Research Fellowship from 1994 to 1999. We greatly acknowledge Papua New Guinea and New Ireland authorities for permission to collect the coral cores and M. McPhaden, PMEL, for use of TAO buoy data. We were greatly appreciative of the volunteer work done by our two divers Bruce Radke and Dieter Burmann who joined us at Kavieng to operate the hydraulic drill. Frederick Taylor from the University of Texas, at Austin, kindly provided the in situ measurements of SST. We thank Steve Eggins for his comments on an early version and Rob Dunbar and other reviewers for their suggestions, which have substantially improved the manuscript.

References

Alibert, C. (1999), Evaluating Sr/Ca and trace elements in *Porites* corals from northern Papua New Guinea as a proxy for SST in the western Pacific warm pool, EUG 10, March 28th–April 1st, 1999, *J. Conf. Abstr.*, *4*(1), B02:2B.

Alibert, C., and L. Kinsley (2008), A 170-year Sr/Ca and Ba/Ca coral record from the western Pacific warm pool: 2. A window into variability of the New Ireland Coastal Undercurrent, *J. Geophys. Res.*, doi:10.1029/2007JC004263, in press.

Alibert, C., and M. T. McCulloch (1997), Strontium/calcium ratios in modern *Porites* corals from the Great Barrier Reef as a proxy for sea surface temperature: Calibration of the thermometer and monitoring of ENSO, *Paleoceanography*, *12*, 345–363.

Alibert, C., L. Kinsley, S. J. Fallon, M. T. McCulloch, R. Berkelmans, and F. McAllister (2003), Sources of trace element variability in Great Barrier Reef corals affected by the Burdekin flood plumes, *Geochim. Cosmochim. Acta*, *67*, 231–246.

Alldredge, A., and M. W. Silver (1988), Characteristics, dynamics and significance of marine snow, *Prog. Oceanogr.*, *20*, 41–82.

Allemand, D., E. Tambutté, J.-P. Girard, and J. Jaubert (1998), Organic matrix synthesis in the scleractinian coral *Stylophora pistillata*: Role in biomineralization and potential target of the organotin tributyltin, *J. Exp. Biol.*, *201*, 2001–2009.

Allison, N., and A. A. Finch (2004), High-resolution Sr/Ca records in modern *Porites lobata* corals: Effects of skeletal extension rate and architecture, *Geochem. Geophys. Geosyst.*, *5*, Q05001, doi:10.1029/2004GC000696.

Arko, R., et al. (2007), The Global Multi-Resolution Topography (GMRT) synthesis, *Eos Trans. AGU*, *88*(52), Fall Meet. Suppl., Abstract IN51B-0405.

Bacon, M. P., and J. M. Edmond (1972), Barium at GEOSECS III in the southwest Pacific, *Earth Planet. Sci. Lett.*, *16*, 66–74.

Beck, J. W., R. L. Edwards, E. Ito, F. W. Taylor, J. Recy, F. Rougerie, P. Joannot, and C. Henin (1992), Sea-surface temperature from coral skeletal strontium/calcium ratios, *Science*, *257*, 644–647.

Butt, J., and E. Lindstrom (1994), Currents off the east coast of New Ireland, Papua New Guinea, and their relevance to regional undercurrents in the western equatorial Pacific Ocean, *J. Geophys. Res.*, *99*, 12,503–12,514.

Cardinal, D., B. Hamelin, E. Bard, and J. Pätzold (2001), Sr/Ca, U/Ca and δ^{18}O records in recent massive corals from Bermuda: Relationships with sea surface temperature, *Chem. Geol.*, *176*, 213–233.

Carton, J. A., B. S. Giese, and S. A. Grodsky (2005), Sea level rise and the warming of the oceans in the Simple Ocean Data Assimilation (SODA) ocean reanalysis, *J. Geophys. Res.*, *110*, C09006, doi:10.1029/2004JC002817.

Chan, L. H., D. Drummond, J. M. Edmond, and B. Grant (1977), On the barium data from the Atlantic GEOSECS expedition, *Deep Sea Res.*, *24*, 613–649.

Clarke, A. J., and A. Lebedev (1996), Long-term changes in equatorial Pacific trade winds, *J. Clim.*, *9*, 1020–1029.

Clausen, C. D., and A. A. Roth (1975), Effect of temperature and temperature adaptation on calcification rate in the hermatypic coral *Pocillopora damicornis*, *Mar. Biol.*, *33*, 93–100.

Cresswell, G. R. (2000), Coastal currents of northern Papua New Guinea, and the Sepik River outflow, *Mar. Freshwater Res.*, *51*, 553–564.

Cronin, M. F., and M. J. McPhaden (1997), The upper ocean heat balance in the western equatorial Pacific warm pool during September–October 1992, *J. Geophys. Res.*, *102*, 8533–8553.

Cruz-Piñón, G., J.-P. Carricart-Ganivet, and J. Espinoza-Avalos (2003), Monthly skeletal extension rates of the hermatypic corals *Montastrea annularis* and *Montastrea faveolata*: Biological and environmental controls, *Mar. Biol.*, *143*, 491–500.

Cuif, J.-P., and Y. Dauphin (2005), The two-step mode of growth in the scleractinian coral skeletons from the micrometre to the overall scale, *J. Struct. Biol.*, *150*, 319–331.

de Villiers, S. (1999), Seawater strontium and Sr/Ca variability in the Atlantic and Pacific oceans, *Earth Planet. Sci. Lett.*, *171*, 623–634.

deVilliers, S., B. K. Nelson, and A. R. Chivas (1995), Biological controls on coral Sr/Ca and δ^{18}O reconstructions of sea surface temperatures, *Science*, *269*, 1247–1249.

Dietzel, M., N. Gussone, and A. Eisenhauer (2004), Co-precipitation of Sr^{2+} and Ba^{2+} with aragonite by membrane diffusion of CO_2 between 10 and 50°C, *Chem. Geol.*, *203*, 139–151.

Esser, B. K., and A. M. Volpe (2002), At-sea high-resolution chemical mapping: extreme barium depletion in North Pacific surface water, *Mar. Chem.*, *79*, 67–79.

Evans, M. N., R. G. Fairbanks, and J. L. Rubenstone (1999), The thermal oceanographic signal of ENSO reconstructed from a Kiritimati Island coral, *J. Geophys. Res.*, *104*, 13,409–13,421.

Fallon, S. J., M. T. McCulloch, and C. Alibert (2003), Examining water temperature proxies in *Porites* corals from the Great Barrier Reef: A cross-shelf comparison, *Coral Reefs*, *22*, 389–404.

Felis, T., G. Lohmann, H. Kuhnert, S. J. Lorenz, D. Scholz, J. Pätzold, S. A. Al-Rousan, and S. M. Al-Moghrabi (2004), Increased seasonality in Middle East temperatures during the last interglacial period, *Nature*, *429*, 164–168.

Ferrier-Pagès, C., J. Witting, E. Tambutté, and K. P. Sebens (2003), Effect of natural zooplankton feeding on the tissue and skeletal growth of the scleractinian coral *Stylophora pistillata*, *Coral Reefs*, *22*, 229–240.

Frankignoul, C., F. Bonjean, and G. Reverdin (1996), Interannual variability of surface currents in the tropical Pacific during 1987–1993, *J. Geophys. Res.*, *101*, 3629–3647.

Goldberg, W. M. (2002), Feeding behavior, epidermal structure and mucus cytochemistry of the scleractinian *Mycetophyllia reesi*, a coral without tentacles, *Tissue Cell*, *34*, 232–245.

Gorsky, G., R. Le Borgne, M. Picheral, and L. Stemmann (2003), Marine snow latitudinal distribution in the equatorial Pacific along 180°, *J. Geophys. Res.*, *108*(C12), 8146, doi:10.1029/2001JC001064.

Grodsky, S. A., and J. Carton (2001), Intense surface currents in the tropical Pacific during 1996–1998, *J. Geophys. Res.*, *106*, 16,673–16,684.

Harrison, D. E., and B. S. Giese (1991), Episodes of surface westerly winds as observed from islands in the western tropical Pacific, *J. Geophys. Res.*, *96*, 3221–3237.

Hartten, L. M. (1996), Synoptic settings of westerly wind bursts, *J. Geophys. Res.*, *101*, 16,997–17,019.

Helmle, K. P., R. E. Dodge, and R. A. Ketcham (2000), Skeletal architecture and density banding in *Diploria Strigosa* by X-ray computed tomography, *Proceedings of the 9th International Coral Reef Symposium*, *Bali, Indonesia, 23–27, 2000*, vol. 1, pp. 365–371, Minist. of the Environ., Indonesian Inst. of Sci., Bali, Indonesia.

Houlbrèque, F., E. Tambutté, and C. Ferrier-Pagès (2003), Effect of zooplankton availability on the rates of photosynthesis, tissue and skeletal growth of the scleractinian coral *Stylophora pistillata*, *J. Exp. Mar. Biol. Ecol.*, *296*, 145–166.

Huyer, A., P. M. Kosro, R. Lukas, and P. Hacker (1997), Upper ocean thermohaline fields near 2°S, 156°E, during the Tropical Ocean-Global Atmosphere-Coupled Ocean-Atmosphere Response Experiment, November 1992 to February 1993, *J. Geophys. Res.*, *102*, 12,749–12,784.

Ioualalen, M., J. Holfort, G. Siedler, W. Zenk, C. Hénin, and J. Picaut (2000), The equatorial west Pacific fresh pool at the end of the La Niña event in October/November 1996, *Geophys. Res. Lett.*, *27*, 1243–1246.

Jeandel, C., B. Dupré, G. Lebaron, C. Monnin, and J.-F. Minster (1996), Longitudinal distributions of dissolved barium, silica and alkalinity in the western and southern Indian Ocean, *Deep Sea Res., Part I*, *43*, 1–31.

Jeandel, C., K. Tachikawa, A. Bory, and F. Dehairs (2000), Biogenic barium in suspended and trapped material as a tracer of export production in the tropical NE Atlantic (EUMELI sites), *Mar. Chem.*, *71*, 125–142.

Johnson, G. C., B. M. Sloyan, W. S. Kessler, and E. McTaggart (2002), Direct measurements of upper ocean currents and water properties across the tropical Pacific during the 1990s, *Prog. Oceanogr.*, *52*, 31–61.

Kalnay, E., et al. (1996), The NCEP/NCAR 40-year reanalysis project, *Bull. Am. Meteorol. Soc.*, *77*, 437–471.

Kessler, W. S., and M. J. McPhaden (1995), The 1991–1993 El Niño in the central Pacific, *Deep Sea Res., Part II*, *42*, 295–333.

Kineke, K., J. Woolfe, S. A. Kuehl, J. D. Milliman, T. M. Dellapenna, and R. G. Purdon (2000), Sediment export from the Sepik River, Papua New Guinea: Evidence for a divergent sediment plume, *Cont. Shelf Res.*, *20*, 2239–2266.

Kinsman, D. J. J., and H. D. Holland (1969), The co-precipitation of cations with Ca CO_3-IV. The co-precipitation of Sr^{2+} with aragonite between 16°C and 96°C, *Geochim. Cosmochim. Acta*, *33*, 1–17.

Kuroda, Y. (2000), Variability of currents off the northern coast of New Guinea, *J. Oceanogr.*, *56*, 103–116.

Kuroda, Y., and M. J. McPhaden (1993), Variability in the western equatorial Pacific Ocean during Japanese Pacific climate study cruises in 1989 and 1990, *J. Geophys. Res.*, *98*, 4747–4759.

Lea, D. W., E. A. Boyle, and G. T. Shen (1989), Coralline barium records temporal variability in equatorial Pacific upwelling, *Nature*, *340*, 373–376.

Liu, W. T., A. Zhang, and J. K. B. Bishop (1994), Evaporation and solar irradiance as regulators of sea surface temperature in annual and interannual changes, *J. Geophys. Res.*, *99*, 12,623–12,637.

Lough, J. M., and D. J. Barnes (1990), Intra-annual timing of density band formation of *Porites* corals from the central Great Barrier Reef, *J. Exp. Mar. Biol. Ecol.*, *135*, 35–57.

Mackey, D. J., J. S. Parslow, F. B. Griffiths, H. W. Higgins, and B. Tilbrook (1997), Phytoplankton productivity and the carbon cycle in the western equatorial Pacific under El Niño and non-El Niño conditions, *Deep Sea Res., Part II*, *44*, 1951–1978.

Mackey, D. J., J. E. O'Sullivan, and R. J. Watson (2002), Iron in the western Pacific: A riverine or hydrothermal source for iron in the Equatorial Undercurrent?, *Deep Sea Res., Part I*, *49*, 877–893.

Maes, C., P. Delecluse, and G. Madec (1998), Impact of westerly wind bursts on the warm pool of the TOGA-COARE domain in an OGCM, *Clim. Dyn.*, *14*, 55–70.

Marshall, A. T., and P. L. Clode (2004), Calcification rate and the effect of temperature in a zooxanthellate and an azooxanthellate scleractinian reef coral, *Coral Reefs*, *23*, 218–224.

Marshall, J. F., and M. T. McCulloch (2001), Evidence of El Niño and the Indian Dipole from Sr/Ca derived SSTs for modern corals at Christmas Island, eastern Indian Ocean, *Geophys. Res. Lett.*, *28*, 3453–3456.

Mayer, D. A., and R. H. Weisberg (1998), El Niño-Southern Oscillation-related ocean-atmosphere coupling in the western equatorial Pacific, *J. Geophys. Res.*, *103*, 18,635–18,648.

McCulloch, M. T., S. Fallon, T. Wyndham, E. Hendy, J. Lough, and D. Barnes (2003), Coral record of increased sediment flux to the inner Great Barrier Reef since European settlement, *Nature*, *421*, 727–730.

McPhaden, M. J. (1999), Genesis and evolution of the 1997–98 El Niño, *Science*, *283*, 950–954.

Meyer, G., J. R. Donguy, and R. K. Reed (1986), Evaporative cooling of the western equatorial Pacific Ocean by anomalous winds, *Nature*, *323*, 523–526.
Morrissey, M. L. (1992), The quality of ship observations in the equatorial western Pacific, in *Proceedings of the International COADS Workshop, Boulder, Colorado, 13–15 January 1992*, edited by H. F. Diaz, K. Wolter, and S. D. Woodruff, pp. 115–126, NOAA Environ. Res. Lab., Climate Res. Div., Boulder, Colo.
Murtugudde, R. G., S. R. Signorini, J. R. Christian, A. J. Busalacchi, C. R. McClain, and J. Picaut (1999), Ocean color variability of the tropical Indo-Pacific basin observed by SeaWiFS during 1997–1998, *J. Geophys. Res.*, *104*, 18,351–18,366.
Picaut, J., and T. Delcroix (1995), Equatorial wave sequence associated with warm pool displacements during the 1986–1989 El Niño–La Niña, *J. Geophys. Res.*, *100*, 18,393–18,408.
Plummer, L. N., and E. Busenberg (1987), Thermodynamics of aragonite-strontianite solid solutions: results from stoichiometric solubility at 25 and 76°C, *Geochim. Cosmochim. Acta*, *51*, 1393–1411.
Quinn, T. M., and D. E. Sampson (2002), A multiproxy approach to reconstructing sea surface conditions using coral skeleton geochemistry, *Paleoceanography*, *17*(4), 1062, doi:10.1029/2000PA000528.
Quinn, T. M., F. W. Taylor, T. J. Crowley, C. Henin, P. Joannot, and Y. Join (1998), A multicentury coral stable isotope record from a New Caledonia coral: Interannual and decadal sea surface temperature variability in the southwest Pacific since 1657 A. D., *Paleoceanography*, *13*, 412–426.
Quinn, T. M., F. W. Taylor, and T. J. Crowley (2006), Coral-based climate variability in the Western Pacific Warm Pool since 1867, *J. Geophys. Res.*, *111*, C11006, doi:10.1029/2005JC003243.
Radenac, M. H., and M. Rodier (1996), Nitrate and chlorophyll distributions in relation to thermohaline and current structures in the western tropical Pacific during 1985–1989, *Deep Sea Res., Part II*, *43*, 725–752.
Rayner, N. A., D. E. Parker, E. B. Horton, C. K. Folland, L. V. Alexander, D. P. Rowell, E. C. Kent, and A. Kaplan (2003), Global analyses of SST, sea ice and night marine air temperature since the late nineteenth century, *J. Geophys. Res.*, *108*(D14), 4407, doi:10.1029/2002JD002670.
Rayner, N. A., P. Brohan, D. E. Parker, C. K. Folland, J. J. Kennedy, M. Vanicek, T. Ansell, and S. F. B. Tett (2005), Improved analyses of changes and uncertainties in sea surface temperature measured in situ since the mid-nineteenth century: The HadSST2 data set, *J. Clim.*, *19*(3), 446–469, doi:10.1175/JCLI3637.1.
Reverdin, G. C., C. Frankignoul, E. Kestenare, and M. J. McPhaden (1994), Seasonal variability in the surface currents of the equatorial Pacific, *J. Geophys. Res.*, *99*, 20,323–20,344.
Reynolds, R. W., N. A. Rayner, T. M. Smith, D. C. Stokes, and W. Wang (2002), An improved in situ and satellite SST analysis for climate, *J. Clim.*, *15*, 1609–1625.
Rickaby, R. E. M., D. P. Schrag, I. Zondervan, and U. Riebesell (2002), Growth rate dependence of Sr incorporation during calcification of *Emiliania huxleyi*, *Global Biogeochem. Cycles*, *16*(1), 1006, doi:10.1029/2001GB001408.
Ryan, J. P., P. S. Polito, P. G. Strutton, and F. Chavez (2002), Unusual large-scale phytoplankton blooms in the equatorial Pacific, *Prog. Oceanogr.*, *55*, 263–285.
Siegel, D. A., J. Carter Ohlmann, L. Vashburn, R. R. Bidigare, C. T. Nosse, E. Fields, and Y. Zhou (1995), Solar radiation, phytoplankton pigments and the radiant heating of the equatorial Pacific warm pool, *J. Geophys. Res.*, *100*, 4885–4891.
Sternberg, E., D. Tang, T.-Y. Ho, C. Jeandel, and F. M. M. Morel (2005), Barium uptake and adsorption in diatoms, *Geochim. Cosmochim. Acta*, *69*, 2745–2752.
Swart, P. K., H. Elderfield, and M. J. Greaves (2002), A high-resolution calibration of Sr/Ca thermometry using the Caribbean coral *Montastrea annularis*, *Geochem. Geophys. Geosyst.*, *3*(11), 8402, doi:10.1029/2002GC000306.
Tesoriero, A. J., and J. F. Pankow (1996), Solid solution partitioning of Sr^{2+}, Ba^{2+}, and Cd^{2+} to calcite, *Geochim. Cosmochim. Acta*, *60*, 1053–1063.
Tsuchiya, M., R. Lukas, R. A. Fine, E. Firing, and E. Lindstrom (1989), Source waters of the Pacific Equatorial Undercurrent, *Prog. Oceanogr.*, *23*, 101–147.
Tudhope, A. W., D. W. Lea, G. H. Shimmield, C. P. Chilcott, and S. Head (1996), Monsoon climate and Arabian Sea coastal upwelling recorded in massive corals from southern Oman, *Palaios*, *11*, 347–361.
Turk, D., M. J. McPhaden, A. J. Busalacchi, and M. R. Lewis (2001), Remotely sensed biological production in the equatorial Pacific, *Science*, *293*, 471–474.
Ueki, I., Y. Kashino, and Y. Kuroda (2003), Observation of current variations off the New Guinea coast including the 1997–1998 El Niño period and their relationship with Sverdrup transport, *J. Geophys. Res.*, *108*(C7), 3243, doi:10.1029/2002JC001611.
Urban, F. E., J. E. Cole, and J. T. Overpeck (2000), Influence of mean climate change on climate variability from a 155-year tropical Pacific coral record, *Nature*, *407*, 958–989.
Vecchi, G. A., and D. E. Harrison (1997), Tropical Pacific sea surface temperature anomalies, El Niño, and equatorial westerly wind events, *J. Clim.*, *13*, 1814–1997.
Wang, B. (1995), Transition from a cold to warm state of the El Niño–Southern Oscillation cycle, *Meteorol. Atmos. Phys.*, *56*, 17–32.
Watson, E. B. (2004), A conceptual model for near-surface kinetic controls on the trace-element and stable isotope composition of abiogenic calcite crystals, *Geochim. Cosmochim. Acta*, *68*, 1473–1488.
Wijesekera, H., and M. C. Gregg (1996), Surface layer response to weak winds, westerly bursts, and rain squalls in the western Pacific Warm Pool, *J. Geophys. Res.*, *101*, 977–997.
Wischow, D. (1999), Sr/Ca- und U/Ca-Thermometrie an Korallen (*Porites lutea*) aus dem Indischen Ozean, Ph.D. diss., Univ. of Göttingen, Germany.
Wyrtki, K. (1974), Equatorial currents in the Pacific 1950 to 1970 and their relations to trade winds, *J. Phys. Oceanogr.*, *4*, 372–380.

C. Alibert and L. Kinsley, Research School of Earth Sciences, Building 61, Mills Road, Australian National University, Acton, ACT, Australia. (c.alibert@anu.edu.au; leslie.kinsley@anu.edu.au)